Supplementary Material for "Improving the Coherence Time of Superconducting Coplanar Resonators"

H. Wang, M. Hofheinz, J. Wenner, M. Ansmann, R. C. Bialczak, M. Lenander, Erik Lucero, M. Neeley, A. D. O'Connell, D. Sank, M. Weides, A. N. Cleland, and John M. Martinis
Department of Physics, University of California, Santa Barbara, California, CA 93106
(Dated: November 17, 2009)

We provide detailed calculations for Ref. [S1], mainly showing how a non-uniform electric field distribution can be accounted for in two-level state dielectric loss.

We consider a coplanar resonator with a non-uniform surface charge distribution, with a cross-section as illustrated in Fig. S1. For the case of identical dielectrics around the resonator metallization, e.g. $\epsilon_1 = \epsilon_2$, we use matrix inversion of the inverse capacitance matrix, defined through the equation in two dimensions

$$V_i = \frac{1}{2\pi\epsilon_1\epsilon_0} \sum_j q_j \ln r_{ij} \ , \tag{S1}$$

to find the surface charge distribution q_j (and thus the field distribution) at position j. Here, V_i is the potential at position i, set to V at the center trace and 0 on ground pads. The separation between elements i and j is r_{ij}, and ϵ_0 is the vacuum permittivity. For $\epsilon_1 \neq \epsilon_2$, the ϵ_1 and ϵ_2 regions can be, respectively, conformally mapped into two rectangles where field distributions are easily calculable [S2]. We find that both approaches yield similar electric field distributions. Note that E fields have tangential components that are continuous at the interface between the two dielectrics. For simplicity, we discuss the results based on uniform dielectrics. Note that these calculations were also checked with commercial software (COMSOL), which were roughly in agreement with our simplified model.

Most of the energy of the E field is concentrated around the gap of the coplanar line. For the $w_c = 5$ μm resonator, for example, $\approx 90\%$ of the metal-oxide surface energy is stored within 1 μm around the gap region. Finite element analysis using COMSOL shows that ≈ 2000 ppm of the total resonator energy is stored in the substrate surface and ≈ 600 ppm is in the metal surface, assuming a thickness of 3 nm and a dielectric constant of 10 for surface layers.

We now calculate the power dependence of the resonator quality factor Q coming from dielectric loss of two-level states (TLS) at the metal surface. We first consider the approximation of a uniform electric field $E_{\text{side wall}}$ coming from the surface region around the middle of the center-trace side wall, as indicated in Fig. S1. From the loss theory of TLS, we find

$$\begin{aligned} 1/Q_{\text{side wall}} &\propto 1/\sqrt{1 + E^2_{\text{side wall}}/E^2_{\text{s}}} \\ &= 1/\sqrt{1 + (\gamma V/w_{\text{g}})^2/E^2_{\text{s}}} \\ &= 1/\sqrt{1 + V^2/V^2_{\text{s}}} \end{aligned} \tag{S2}$$

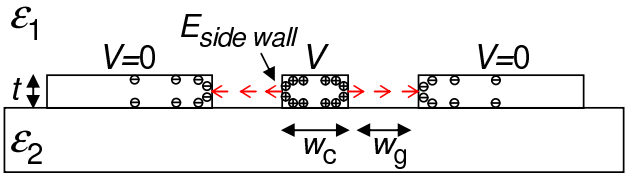

FIG. S1: Cross-section of a coplanar resonator showing the center trace width w_c, the gap separation w_g between the center trace and the ground plane, and the metal film thickness t. The substrate has a dielectric constant ϵ_2 and the region above is ϵ_1. The potential difference between the center trace and ground plane is V. $E_{\text{side wall}}$ around the middle point of the center-trace side wall is indicated.

where E_{s} is the saturation field for the TLS, and $\gamma = E_{\text{side wall}}/(V/w_{\text{g}})$ is a factor obtained from numerical simulations (Eq. S1) and tabulated for three common parameter sets in Table S1. An exact relation is obtained by incorporating the computed field distribution and using a weighted sum of the TLS loss over all exposed metal surfaces

$$1/Q_{\text{exact}} \propto \sum_i \frac{1}{\sqrt{1 + E_i^2/E_{\text{s}}^2}} \cdot \frac{E_i^2}{\sum_i E_i^2} \ , \tag{S3}$$

where the surface fields E_i are proportional to the resonator voltage V.

In Fig. S2 we plot Q_{exact} (dots) versus V/V_{s} for a resonator with $w_c = 5$ μm, using the exact field distribution from Eqs. S1 and S3. For reference, $Q_{\text{side wall}}$ from Eq. S2 is also plotted as the blue line. To more simply describe the results of the numerical calculations, we fit a line to the dots at the low voltage region according to

$$1/Q_{\text{exact}} \propto 1/\sqrt{1 + (V/\alpha V_{\text{s}})^{\beta}}, \tag{S4}$$

TABLE S1: Fitting and scaling parameters obtained from numerical calculations based on Eqs. S1, S2 and S4, as explained in text.

w_c (μm)	w_g (μm)	α	β	γ
5	2	1.31	1.64	2.40
8	3.2	1.40	1.59	2.93
16	6.4	1.48	1.56	3.85

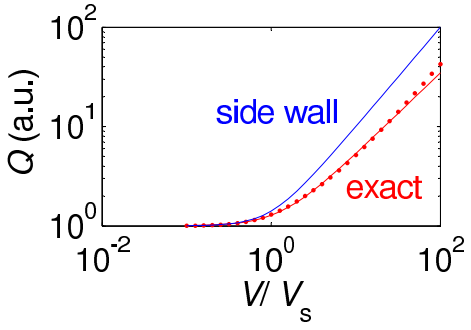

FIG. S2: Q versus V/V_s for both a uniform field around the center-trace side wall (blue line, Eq. S2) and an exact field distribution over all exposed metal surfaces (red dots, Eq. S3). Red line passing through dots is a fit using Eq. S4.

where α and β are rescaling factors, obtained from the fits, that are also listed in Table S1. Accordingly, we use $\beta = 1.6$ to fit the experimental data of Q_m versus V (or V_{rms} as in Ref. [S1]) such that

$$\frac{1}{Q_m} = \frac{1}{Q_0} + \frac{1}{Q_{TLS}} \cdot \frac{1}{\sqrt{1+(V/V_s')^{1.6}}}, \qquad \text{(S5)}$$

with Q_0, Q_{TLS}, and V_s' as fitting parameters. These fit parameters are listed in Table S2. We find that varying β slightly does not affect the systematic trend of Q_0 and Q_{TLS}, as shown in Fig. 3(c) in Ref. [S1].

From the fitted V_s' we obtain the saturation field for the metal surface layer as

$$E_s = \frac{\gamma V_s'}{\alpha w_g}. \qquad \text{(S6)}$$

In Table S2 we list the fitted saturation fields E_s's from different resonators. They are reasonably close to each other. It is also noted that the estimated E_s's for metal surface oxide are within an order of magnitude of those for plasma-enhanced chemical vapor deposition (PECVD) grown SiO_2 and SiN (see Refs. [S3, S4, S5]).

Q_0 is the power-independent term from a fit, which is related to the electrical loading through coupling capacitors, the vortex loss, the radiation loss depending on the resonator geometry, the non-equilibrium quasiparticle loss, and possibly other unknown loss mechanisms. It is possible that Q_0 may also be partly from the surface layer of the sapphire substrate, for which the saturation field might be significantly higher than E_s's listed in Table S2. Support of this hypothesis is that Q_0 also increases with increasing w_g. However, we could not meaningfully extract a saturation field for this background dissipation. We tried fitting the data with two E_s's of different magnitudes to account for this effect, but it was unsuccessful as it introduced too many degrees of freedom for the limited number of data points. Singling out the substrate surface TLS contribution to Q_0 will require further measurements.

TABLE S2: Parameters from fits to the Q_m versus V (or V_{rms}) data (Fig. 3 in Ref [S1]), according to Eqs. S5 and S6.

	w_c (μm)	w_g (μm)	Q_0 (10^5)	Q_{TLS} (10^5)	V_s' (10^{-5} V)	E_s (V/m)
	5	2	3.16	1.23	5.0	46
Al	8	3.2	3.85	1.41	5.4	35
	16	6.4	4.39	2.92	11.8	48
	5	2	2.79	2.82	6.0	55
Re	8	3.2	3.33	5.43	7.8	51
	16	6.4	5.84	8.41	10.7	43

We have shown that the surface TLS model can interpret the data of the power dependence of Q_m by introducing three parameters Q_0, Q_{TLS}, and E_s. The resulting fitting values of these three parameters are reasonable and can be a useful guidance for future experiments. However, we do not exclude other explanations of the experimental data.

Finally we comment on the connection between results from the power measurement (Fig. 3 in Ref. [S1]) and the temperature measurement (Fig. 2 in Ref. [S1]). It has been shown in previous studies (see references in Ref. [S1]) that a downturn in resonance frequency at temperatures below $T_c/10$ indicates the existence of surface TLS. This feature is missing in our data presumably because we use lower T_c materials (1 K versus 10 K). At the lowest temperatures, the TLS loss mechanism is not dominant (though important) as Q_0 and Q_{TLS} are comparable (see Table S2). Measurements of temperature dependence are mostly consistent with quasiparticle dissipation.

Acknowledgements. Devices were made at the UCSB Nanofabrication Facility, a part of the NSF-funded National Nanotechnology Infrastructure Network. This work was supported by IARPA under grant W911NF-04-1-0204 and by the NSF under grant CCF-0507227.

[S1] H. Wang, M. Hofheinz, J. Wenner, M. Ansmann, R. C. Bialczak, M. Lenander, E. Lucero, M. Neeley, A. D. O'Connell, D. Sank, M. Weides, A. N. Cleland, and J. M. Martinis, arXiv:0909.0547.

[S2] J. Gao, Ph.D. thesis, California Institute of Technology (2008).

[S3] A. D. O'Connell, M. Ansmann, R. C. Bialczak, M. Hofheinz, N. Katz, E. Lucero, C. McKenney, M. Neeley, H. Wang, E. M. Weig, A. N. Cleland, and J. M. Martinis, Appl. Phys. Lett. **92**, 112903 (2008).

[S4] J. M. Martinis, K. B. Cooper, R. McDermott, M. Steffen, M. Ansmann, K. D. Osborn, K. Cicak, S. Oh, D. P. Pappas, R. W. Simmonds, and C. C. Yu, Phys. Rev. Lett. **95**, 210503 (2005).

[S5] J. Gao, J. Zmuidzinas, B. A. Mazin, H. G. Leduc, and P. K. Day, Appl. Phys. Lett. **90**, 102507 (2007).